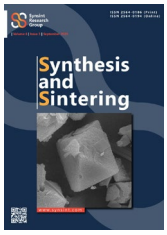
Available online at www.synsint.com

Synthesis and Sintering

ISSN 2564-0186 (Print), **ISSN** 2564-0194 (Online)



Research article

Effect of welding polarity on iron dilution, clad chemistry, and interfacial microstructure in multilayer SMAW Inconel 625 overlays on SA-387 grade 11 steel

Majid Haghighi Borujeni [a], Iman Mohammadi [b], Fardin Nematzadeh [c,*]

[a] *Material Expert, Machine Sazi Arak, Arak, Iran*
[b] *Head of Welding and Material Department, Machine Sazi Arak, Arak, Iran*
[c] *Department of Advanced Materials, Materials and Energy Research Center, Karaj, Iran*

ABSTRACT

High-strength steels used in the oil and gas industry are susceptible to corrosion in harsh environments. Although Inconel 625 offers excellent corrosion resistance, its high cost limits large-scale application. Weld cladding with Inconel 625 provides a cost-effective alternative; however, excessive dilution with the steel substrate increases iron content and degrades clad chemistry. This study investigates the effect of welding polarity on iron dilution and clad chemistry in multilayer SMAW Inconel 625 overlays deposited on SA-387 grade 11 steel. Three-layer claddings were produced using direct current electrode negative (DCEN) and direct current electrode positive (DCEP) polarities. Clad chemistry was characterized by positive material identification (PMI) and scanning electron microscopy with energy-dispersive X-ray spectroscopy (SEM-EDS). Iron dilution was calculated from measured iron contents. Under the investigated conditions, the DCEN clad exhibited substantially lower iron content (3.97 ± 0.12 wt%) compared with the DCEP clad (10.6 wt%). DCEN also permitted a lower welding current (100–120 A versus 140–150 A for DCEP), resulting in reduced heat input. These findings demonstrate that DCEN polarity can effectively minimize iron dilution and produce clad chemistry closer to that of the Inconel 625 filler metal. Corrosion performance was not directly evaluated in this study and remains a subject for future investigation.
© 2026 The author(s) retain the copyright and full publishing rights.

KEYWORDS

Dilution
Inconel 625
Weld cladding
Polarity

OPEN ACCESS

1. Introduction

Weld cladding is widely used to improve the surface properties of steels exposed to severe service environments, particularly in the oil and gas, petrochemical, power generation, and pressure-vessel industries. Nickel-based alloys such as Inconel 625 are frequently selected as cladding materials because of their excellent corrosion resistance, mechanical properties, and suitability for demanding service environments. The performance of an Inconel 625 overlay is strongly influenced by the deposition process, welding parameters, dilution, and the resulting microstructure and chemical composition of the clad layer [1–5]. Therefore, controlling the interaction between the deposited alloy and the steel substrate is essential for obtaining a sound overlay with an appropriate chemical composition and corrosion-resistant surface.

Several welding processes have been employed to deposit Inconel 625 overlays, including gas metal arc welding (GMAW), plasma transferred arc (PTA), flux-cored arc welding (FCAW), gas tungsten

* Corresponding author. *E-mail address:* f.nematzadeh@merc.ac.ir (F. Nematzadeh)
Received 21 May 2026; Received in revised form 2 September 2026; Accepted 3 September 2026.
This is an open access article under the CC BY license (https://creativecommons.org/licenses/by/4.0/). Published by Synsint Research Group.
https://doi.org/10.53063/synsint.2026.63343

arc welding (GTAW), and cold metal transfer (CMT) processes [1, 3, 6–10]. Previous studies have demonstrated that welding parameters and process conditions can significantly affect the geometry, microstructure, chemical composition, and corrosion behavior of Inconel 625 overlays [1, 6–10]. In particular, alloy 625 overlays deposited on carbon and low-alloy steels have been investigated with respect to microstructure, mechanical behavior, and processing conditions [11, 12]. Moradi and Ketabchi [11] investigated alloy 625 weld overlays deposited on ASTM A516 grade 70 carbon steel and reported an austenitic dendritic weld-metal microstructure together with acceptable shear strength at the clad interface. Elango and Balaguru [12] investigated Inconel 625 overlay deposition on carbon steel using GMAW and emphasized the importance of controlling weld chemistry, particularly the Fe content of the deposited overlay.

Among the available deposition processes, shielded metal arc welding (SMAW) remains attractive for field and repair applications because of its relatively simple equipment, portability, and suitability for depositing overlays on large or complex components. The welding current and electrode polarity are important parameters in SMAW because they influence arc characteristics, heat distribution, penetration, and bead geometry [13–15]. Previous investigations have reported differences in weld penetration, bead geometry, microstructure, and residual stress under direct-current electrode-positive (DCEP) and direct-current electrode-negative (DCEN) conditions [14, 15]. These effects are particularly important in cladding applications because changes in penetration directly influence the extent of substrate melting and, consequently, dilution of the deposited alloy.

For multilayer nickel-based overlays, iron dilution is a particularly important parameter because the deposited material is progressively mixed with the steel substrate during welding. Excessive iron incorporation can alter the chemical composition of the overlay and reduce the relative concentration of alloying elements characteristic of Inconel 625. The effects of dilution on the microstructure and properties of Ni-based alloy 625 coatings have been reported in previous studies [16, 17]. Investigations of Inconel 625 overlays on carbon and low-alloy steels have likewise shown that substrate composition and welding parameters influence the chemical composition and microstructure of the deposited layer [18, 19].

The influence of welding current on Inconel 625 overlays has been specifically investigated by Antoszczyszyn et al. [20], who demonstrated that increasing deposition current increased dilution and affected the resulting microstructure and properties of the coating. Song et al. [21] investigated the effect of welding current on the Inconel 625/X65 cladding interface and reported that increasing welding current, and consequently heat input and arc force, increased dilution and modified the composition transition region and microstructure near the interface. These findings indicate that controlling welding conditions is essential for limiting substrate melting and maintaining the desired composition of the overlay.

The relationship between iron dilution and the corrosion performance of Inconel 625 overlays has also received considerable attention. Cunha et al. [2] investigated the effect of iron dilution on the corrosion resistance of Inconel 625 welding overlays deposited on carbon steel, demonstrating the importance of controlling dilution when evaluating overlay performance. Xu et al. [17] examined the intergranular corrosion behavior of Inconel 625 deposited by CMT/GTAW and demonstrated the relationship between deposition conditions, microstructure, and corrosion behavior. These studies indicate that the interaction between the steel substrate and nickel-based overlay can substantially influence the final chemical and microstructural characteristics of the deposited material.

Microstructural and corrosion investigations of Inconel 625 overlays deposited by different processes have further demonstrated the importance of the deposition procedure. Studies using PTA and related processes have evaluated the influence of welding parameters on the geometry, microstructure, corrosion behavior, and pitting resistance of Inconel 625 coatings [6–9]. Kumar et al. [18] evaluated the microstructure and corrosion behavior of Inconel 625 and Inconel 82 overlays on 304L stainless steel weld metal and reported a fully austenitic microstructure in the Inconel overlays together with improved corrosion performance of Inconel 625 in the investigated media. The effects of heat treatment on steel/Inconel 625 coating systems have also been investigated. Trindade et al. [19] studied a C-Mn steel/Inconel 625 coating system and demonstrated that different heat-treatment routes could modify the microstructure and microhardness of the coated system. These findings emphasize that both the as-deposited condition and subsequent thermal history can influence the final characteristics of an Inconel 625 overlay.

Several studies have specifically investigated the performance of Inconel 625 overlays produced using different welding processes. Alvarães et al. [9] evaluated the performance of Inconel 625 weld overlays obtained by FCAW, while Costa et al. [1] investigated the microstructure of Inconel 625 cladding deposited by GMAW and GMAW with a rotating electrode. Macedo et al. [4] studied the effects of shielding gas and substrate thickness on dilution and microstructure in Inconel 625 MIG/MAG coatings. These studies demonstrate that process-related parameters can substantially influence dilution and microstructural development in nickel-based overlays.

Heat input is another important factor governing dilution and microstructural evolution during overlay welding. Changes in welding current and other heat-input-related parameters can modify substrate melting, penetration, solidification conditions, and the resulting microstructure of the deposited alloy [16, 20, 21]. Kim et al. [16] investigated the effect of heat input on the pitting resistance of Inconel 625 welds produced by overlay welding, while Nachimuthu et al. [22] examined the high-temperature corrosion performance of Inconel 625 hard overlays deposited on stainless steel substrates. These studies emphasize the importance of controlling the thermal conditions during deposition to obtain a suitable combination of chemical composition, microstructure, and corrosion resistance.

For industrial overlay applications, welding procedure qualification and control of weld quality are also essential. Welding standards provide requirements and guidance concerning welding variables, qualification procedures, materials, and inspection practices [15, 23, 24]. In addition, previous investigations have examined the influence of welding polarity on weld geometry and penetration and have demonstrated that electrode polarity can substantially affect the characteristics of deposited weld metal [15]. These considerations are particularly important for SMAW overlays, where changes in polarity can alter arc behavior, heat distribution, and substrate melting.

Recent studies have also explored alternative processes for depositing Inconel 625 overlays and improving their resistance to corrosion and environmentally assisted cracking. Cold metal transfer (CMT), for example, has been used to fabricate Inconel 625/X80 overlays with controlled microstructures and resistance to sulfide stress corrosion

Table 1. Chemical composition of the base metal and welding electrode (wt%).

Material	Base metal	Inconel 625
C	0.15	0.025
Si	0.57	0.4
Mn	0.51	0.7
Cr	1.27	22
Ni	0.04	≥60.0
Mo	0.51	9
Al	≤ 0.03	≤ 0.4
Nb	0.002	3.3
S	≤ 0.001	–
P	≤ 0.005	–
Fe	≥60.0	0.5

cracking [17,25]. Other investigations have reported the effects of process parameters on Inconel 625 coatings and the resulting microstructural and corrosion characteristics [1, 3, 4, 6, 8, 10, 13–17]. Although these advanced processes can provide improved control over heat input and dilution, SMAW remains an important practical option for applications where equipment simplicity, accessibility, and repair capability are major considerations.

Despite the extensive research on Inconel 625 weld overlays, relatively limited attention has been given to the specific influence of welding polarity on iron dilution during multilayer SMAW deposition of Inconel 625 on SA-387 grade 11 class 2 steel. This substrate is relevant to pressure-vessel and high-temperature service applications, where maintaining a corrosion-resistant nickel-based surface while limiting iron incorporation from the substrate is important. Although previous studies have investigated welding polarity, dilution, microstructure, corrosion behavior, and the influence of welding parameters separately [2, 6, 10–15, 17, 26, 27], the combined effect of polarity and multilayer deposition conditions on iron dilution in SMAW Inconel 625 overlays on SA-387 grade 11 class 2 steel requires further investigation.

Accordingly, the present study investigates the effect of welding polarity on iron dilution, clad chemistry, and interfacial microstructure in multilayer SMAW Inconel 625 overlays deposited on SA-387 grade 11 class 2 steel. Preliminary welding trials were performed to identify suitable welding conditions for minimizing iron dilution, followed by detailed characterization of the elemental distribution across the clad layer and the substrate–cladding interface. Particular attention was given to the effects of DCEN and DCEP polarity, welding current, penetration, heat input, and the number of deposited layers. The objective is to identify welding conditions capable of producing a multilayer Inconel 625 overlay with reduced iron dilution and a chemical composition closer to that of the filler metal, thereby providing a basis for improved control of corrosion-resistant weld cladding in industrial applications.

Table 2. Mechanical properties of the base metal and welding electrode.

Material	Base metal	Inconel 625
Temperature (°C)	25	25
Yield strength (MPa)	418	375
Tensile strength (MPa)	585	1440
Elastic modulus (GPa)	210	197
Poisson's ratio	0.289	0.278

2. Materials and methods

The experimental work was carried out at Machine Sazi Arak Company (MSA), Iran. Inconel 625 weld cladding was deposited on SA-387 grade 11 class 2 steel plates using the shielded metal arc welding (SMAW) process to investigate the effect of welding polarity on iron dilution in the deposited overlay.

SA-387 grade 11 class 2 steel, which is widely used in pressure vessels, wellhead equipment, and oil and gas processing facilities operating at elevated temperatures, was selected as the substrate material. Its chemical composition and mechanical properties are presented in Tables 1 and 2, respectively.

Test coupons with dimensions of 150 mm × 150 mm × 35 mm were prepared in accordance with ASME Boiler and Pressure Vessel Code, Section IX (QW-214.2, Figure QW-462.5(e), and Table QW-453). Before welding, the specimens were preheated to 120 °C, as required for P-No. 4 materials by ASME Section IX.

An AWS ENiCrMo-3 electrode with a diameter of 4 mm was used to deposit the corrosion-resistant overlay by the SMAW process. A total of 24 weld passes were applied to achieve an average clad thickness of approximately 8 mm. The welding parameters employed in this study are summarized in Table 3.

Following welding, the clad specimens were subjected to non-destructive testing (NDT) to verify weld integrity and detect any surface or internal discontinuities. Subsequently, post-weld heat treatment (PWHT) was performed in accordance with the requirements of the ASME Boiler and Pressure Vessel Code, Section VIII, Division 1.

3. Results and discussion

3.1. Experimental measurement of iron dilution

To determine the optimum welding parameters for minimizing iron dilution, a series of preliminary cladding trials was performed using test coupons fabricated from the same material as the main specimens. Considering the electrode manufacturer's recommended current range (110–140 A), different welding currents, polarities, and numbers of deposited layers were evaluated, as summarized in Table 3.

The iron content of the deposited overlays was measured using a portable PMI analyzer. Among the investigated conditions, the three-layer cladding produced using direct current electrode negative (DCEN) at a welding current of 110–120 A exhibited the lowest iron dilution. Consequently, these parameters were selected for the subsequent experimental work.

Table 3. Welding parameters and process conditions employed for cladding.

Layer No.	Welding current (A)	Polarity	Voltage (V)	Travel speed (mm/s)	Preheating temp. (°C)	Interpass temp. (°C)	Weld bead dimensions (mm)	Peak temp. (°C)*
1	110–120	DCEN	30–40	3.7–4.7	120	—	15×8×3	567
2	110–120	DCEN	30–40	3.7–4.7	—	180	15×8×3	505
3	110–120	DCEN	30–40	3.7–4.7	—	190	15×8×3	500

* A distance of 7 mm from the weld line centerline. Thermocouples were insulated directly on the base metal at a distance of 7 mm from the weld line, so in the first layer the maximum temperature was detected, and in the second and third layers the existing Inconel on the base metal caused lower temperature readings.

The lower iron dilution obtained with DCEN in the present study can be attributed to the combined effects of welding polarity and the associated welding parameters. Under the investigated conditions, DCEN enabled cladding at a lower welding current than DCEP. Since the calculated heat input depends on welding current, arc voltage, and travel speed, the lower welding current used with DCEN resulted in a lower calculated heat input. In addition, shallower penetration was observed with DCEN compared with DCEP, which limited the melting and mixing of the steel substrate with the deposited alloy and consequently reduced the amount of iron incorporated into the clad layer. Therefore, the lower dilution observed with DCEN should be considered a result of the combined effects of polarity, welding current, heat input, and penetration rather than polarity alone.

The greater penetration observed under DCEP conditions is consistent with the findings reported by Kumar et al. [14] and Aloraier et al. [15], who also reported differences in penetration between DCEP and DCEN under SMAW conditions. However, penetration characteristics are affected by several interacting factors, including welding polarity, welding current, arc voltage,



Fig. 1. a) Clad specimens prepared under various welding conditions and b & c) chemical composition measurements using a portable positive material identification (PMI) analyzer: b) Three-layer DCEP and c) three-layer DCEN.

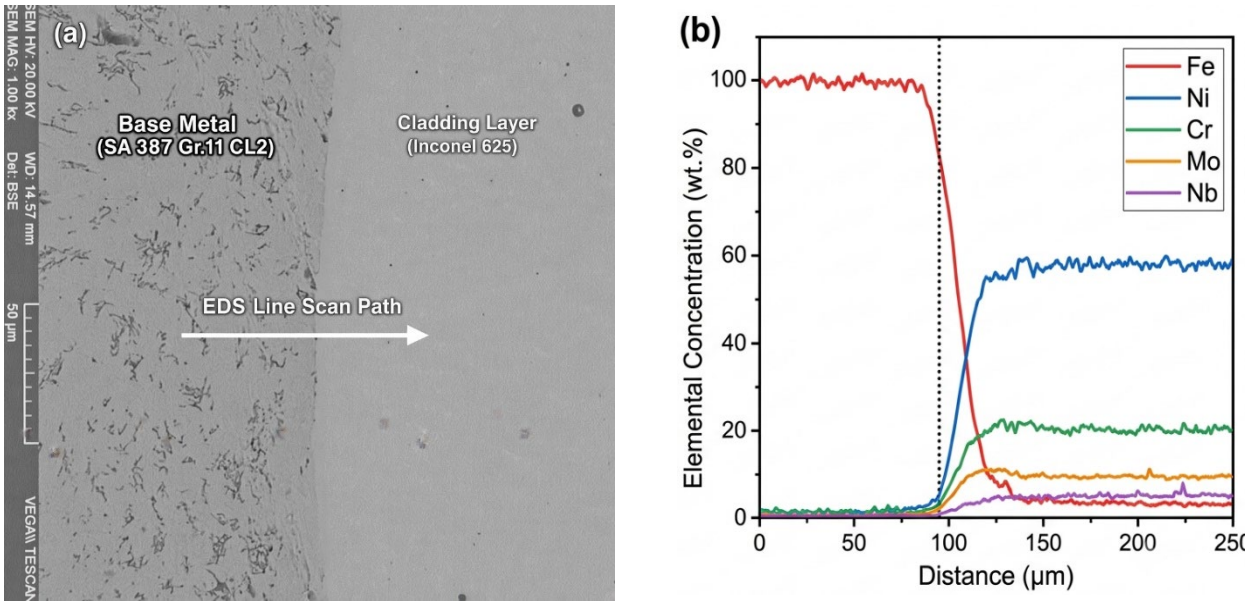


Fig. 2. Scanning electron microscopy (SEM) micrograph and corresponding EDS line scan analysis across the interface: base metal on the left and cladding layer on the right.

travel speed, electrode characteristics, and heat distribution. Under the conditions investigated in the present study, the shallower penetration obtained with DCEN reduced substrate melting and consequently contributed to lower iron dilution. The lower welding current associated with DCEN also resulted in a lower calculated heat input, which further contributed to limiting substrate melting.

From a practical standpoint, the selected DCEN condition provided satisfactory arc stability while allowing the required clad thickness to be deposited at a lower welding current. The lower dilution achieved under these conditions is beneficial for controlling the incorporation of iron from the steel substrate into the Inconel 625 overlay. Accordingly, under the welding conditions investigated in this study, DCEN represents a suitable polarity for multilayer Inconel 625 cladding when minimizing iron dilution is a primary objective.

Among all the investigated conditions, specimen No. 5 exhibited the lowest iron dilution (Table 4). This result can be attributed to the combined effects of DCEN polarity and the three-layer cladding sequence, which produced an overall clad thickness of approximately 8 mm. The successive deposition of multiple layers reduced the influence of substrate dilution on the outer clad region, allowing its chemical composition to more closely approach that of the Inconel 625 filler metal. This finding further demonstrates the importance of both welding parameters and cladding thickness in controlling iron dilution in multilayer overlays.

3.2. Elemental distribution and iron dilution across the clad layer

To characterize the elemental distribution across the clad layer, energy-dispersive X-ray spectroscopy (EDS) line-scan analysis was performed. The analysis was carried out along a line extending from the substrate through the substrate–cladding interface to the outer surface of the clad layer. The corresponding elemental profiles are presented together with the scanning electron microscopy (SEM) micrograph of the interface in Fig. 2.

Table 4. Welding parameters and measured Fe content of the preliminary trial specimens.

Specimen No.	Polarity	Current (A)	No. of layers	Clad thickness (mm)	PMI Fe content (wt%)	EDS point 1 (wt%)	EDS point 2 (wt%)	EDS point 3 (wt%)	EDS mean ± SD* (wt%)
1	DCEP	140–150	1	3	22.00	—	—	—	—
2	DCEP	140–150	2	6	12.00	—	—	—	—
3	DCEP	120–125	3	8	10.00	—	—	—	—
4	DCEN	100–120	2	6	7.00	—	—	—	—
5	DCEN	100–120	3	8	3.90	3.9	4.1	3.9	3.97 ± 0.12

* SD: Standard deviation

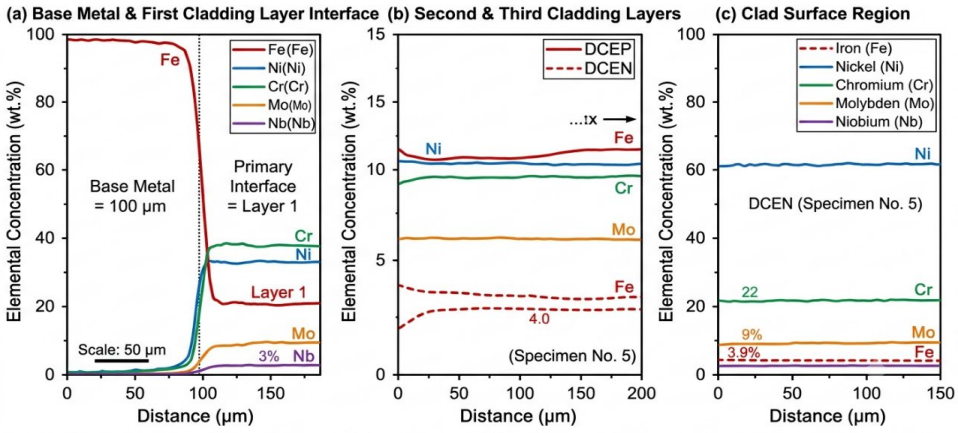


Fig. 3. EDS line scan profile across the interface showing elemental concentration (wt%) on the vertical axis versus distance (μm) on the horizontal axis: a) base metal and first cladding layer, b) second and third cladding layers, and c) top surface of the cladding.

As shown in Fig. 3, the concentrations of nickel (Ni), chromium (Cr), and molybdenum (Mo) gradually increase with increasing distance from the substrate toward the clad surface, whereas the iron (Fe) concentration decreases correspondingly. This compositional gradient reflects the progressive reduction in dilution from the carbon steel substrate as successive clad layers are deposited. Near the outer surface of the overlay, the Fe content reaches its minimum while the concentrations of the principal alloying elements approach those of the Inconel 625 filler metal, indicating effective control of iron dilution in the final clad layer.

Several mathematical formulations have been proposed to quantify iron dilution in weld cladding. In the present study, the dilution percentage was calculated using Eq. 1, which has been widely adopted in the literature [9].

$$\text{Dilution}(\%) = \frac{\rho_s(Fe_c - Fe_{w/p})}{\rho_s(Fe_c - Fe_{w/p}) + \rho_w(Fe_s - Fe_c)} \times 100 \quad (1)$$

where ρ_s = 7.80 gr/cm^3 and ρ_w = 8.44 gr/cm^3 are the densities of the substrate and the filler metal, respectively.

Fe_s = 96.9% and Fe_c extracted from EDS (Fig. 4) represent the iron contents (wt%) of the substrate and the clad layer, whereas $Fe_{W/P}$ = 0.5% denotes the iron content of the filler wire (or powder).

The iron concentration in the clad layer was determined by SEM-EDS area-scan analysis performed at both the substrate–cladding interface and the outer surface of the overlay, as shown in Figs. 3 and 4. The iron dilution percentages calculated using the PMI and EDS techniques are summarized in Tables 6 and 7, respectively, based on Eq. 1.

In these tables, the numerical suffixes (1, 2, and 3) indicate the number of deposited clad layers, while the accompanying abbreviations identify the welding polarity employed during deposition.

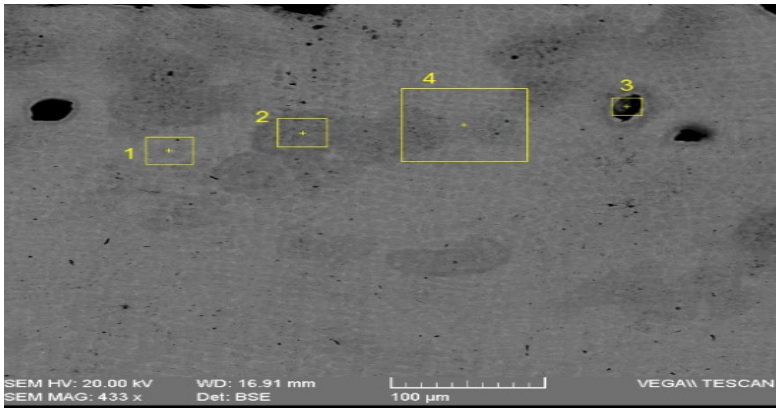


Fig. 4. Representative EDS elemental spectrum and surface quantitative chemical analysis acquired from the top cladding layer of specimen No. 5.

Table 5. Measured elemental concentration (wt%) obtained from EDS line scan analysis from the base metal to the third cladding layer.

Element	Mo (wt%)	Nb (wt%)	Ni (wt%)	Fe (wt%)	Cr (wt%)	C*
Point 1	0.00	0.00	0.00	94.20	0.00	31
Point 2	0.00	0.00	43.75	43.75	17.50	20
Point 3	5.43	3.26	54.35	19.57	17.39	8
Point 4	6.59	4.40	47.25	18.68	16.48	9
Point 5	8.60	4.30	62.37	8.60	18.28	7
Point 6	7.87	5.62	66.29	7.87	19.10	11
Point 7	9.78	4.35	61.96	5.43	19.57	8
Point 8	8.79	4.40	64.84	3.85	20.88	9

* C values are the originally measured EDS values and are not included in the normalized composition.

Table 6. Evaluation of the iron dilution percentage calculated using PMI analysis data and the dilution formulation.

Welding condition (No. of layers/polarity)	Measurement location	Dilution (%)
1-DCEP	Clad surface	22.6
2-DCEP	Clad surface	11.7
3-DCEP	Clad surface	10.6
2-DCEN	Clad surface	7.3
3-DCEN	Clad surface	3.9

Table 7. Evaluation of the iron dilution percentage calculated using EDS analysis data and the dilution formulation.

Welding condition (No. of layers/polarity)	Measurement location	Dilution (%)
3-DCEN	Base metal (fusion line)	78.6
3-DCEN	Base metal (fusion line)	73.7
3-DCEN	Base metal (fusion line)	68.6
3-DCEN	Base metal (fusion line)	37.7
3-DCEN	First layer (layer 1)	19.4
3-DCEN	First layer (layer 1)	18.3
3-DCEN	Second layer (layer 2)	8.4
3-DCEN	Second layer (layer 2)	7.3
3-DCEN	Clad surface	5.1
3-DCEN	Clad surface	3.4

4. Conclusions

The effects of welding polarity on iron dilution during SMAW cladding of Inconel 625 onto ASME SA-387 grade 11 class 2 steel were investigated. Based on the experimental results, the following conclusions can be drawn:

- **Optimization of dilution:** Preliminary welding trials demonstrated that a three-layer cladding sequence deposited using direct current electrode negative (DCEN) polarity at a welding current of 110–120 A produced the lowest iron dilution, approximately 3.97 wt%.
- **Effect of welding polarity:** DCEN consistently produced lower iron dilution than DCEP. The reduced dilution was associated with shallower weld penetration, resulting in less melting of the substrate and a lower amount of iron incorporated into the deposited overlay.
- **Influence of heat input:** Under the welding conditions investigated in this study, the lower welding current used with DCEN resulted in a lower calculated heat input, which, together with the observed shallower penetration, contributed to limiting base metal melting and reducing iron dilution.
- **Effect of cladding thickness:** Increasing the number of deposited layers reduced the influence of substrate dilution on the outer clad region. The three-layer overlay, with an average thickness of approximately 8 mm, produced the lowest iron concentration in the outer clad layer, allowing its chemical composition to more closely approach that of the Inconel 625 filler metal. This result indicates that increasing the cladding thickness can effectively reduce the influence of substrate dilution on the chemical composition of the outer clad layer.
- **Industrial significance:** The results demonstrate that combining DCEN polarity with a three-layer cladding sequence can produce Inconel 625 weld overlays with low iron dilution and a chemical composition closer to that of the filler metal. The measured iron content of the outer clad layer satisfies the iron-content requirement specified by Petrobras N-1707 for corrosion-resistant weld overlays. However, since corrosion testing was not performed in the present study, the corrosion performance of the deposited overlay was not directly evaluated. Therefore, the present findings indicate the potential applicability of the proposed welding procedure for corrosion-resistant overlay applications, while further corrosion testing is required to confirm its corrosion performance.

CRediT authorship contribution statement

Majid Haghighi Borujeni: Data curation, Formal analysis, Validation, Visualization, Writing – original draft.
Iman Mohammadi: Methodology, Project administration, Writing – review & editing.
Fardin Nematzadeh: Conceptualization, Methodology, Supervision.

Data availability

The data underlying this article will be shared on reasonable request to the corresponding author.

Declaration of competing interest

The authors declare no competing interests.

Funding and acknowledgment

The experimental work presented in this study was carried out at Machine Sazi Arak Company (MSA), Iran. The authors gratefully acknowledge the technical and financial support provided by MSA, particularly the Equipment Manufacturing Group, the Welding and Materials Department, and the Central Laboratories. The authors also express their sincere appreciation to the Department of Advanced Materials, Materials and Energy Research Center, Iran, and their academic supervisors for their invaluable guidance and continuous support throughout this research.

References

[1] J.F.M. Costa, J.C.F. Jorge, L.F.G. de Souza, M.C. Mendes, H.N. Farneze, H.A.Y. Magalhães, Microstructural evaluation of Inconel 625 weld cladding deposited by the GMAW and GMAW with rotating electrode processes, Technol. Metal. Mater. Min. 21 (2024) e2848. https://doi.org/10.4322/2176-1523.20242848.
[2] A.B. Cunha, J. Vatavuk, C.R.C. Lima, Investigating the effects of iron dilution on the corrosion resistance of Inconel 625 welding overlay on carbon steel, Materials. 18 (2025) 5574. https://doi.org/10.3390/ma18245574.
[3] M. Rozmus-Górnikowska, M. Blicharski, J. Kusiński, Influence of weld overlaying methods on microstructure and chemical composition of Inconel 625 boiler pipe coatings, Kovove Mater. 52 (2014) 141–147. https://doi.org/10.4149/km-2014-3-141.
[4] R.J. Macedo, C. de Azevedo Celente, D. Souza, H.L. Costa, Effects of the shielding gas and substrate thickness on dilution and microstructure of Inconel® 625 MIG/MAG welded coatings, J. Braz. Soc. Mech. Sci. Eng. 46 (2024) 458. https://doi.org/10.1007/s40430-024-05041-3.
[5] J.T.M. de Hosson, J.L. de Mol van Otterloo, Surface engineering with lasers: Application to Co-based materials, Surf. Eng. 13 (1997) 471–481. https://doi.org/10.1179/sur.1997.13.6.471.
[6] P.P.B. da Silva, I. dos Santos Araújo, M.R.S. Vieira, S.L. Urtiga Filho, Influence of welding parameters on the geometric and microstructural characteristics of Inconel 625 coatings deposited on ASTM A36 steel by plasma transferred arc, Matéria. 25 (2020) e1050. https://doi.org/10.1590/S1517-707620200002.1050.
[7] R.A. Lorenzoni, R.P. Gasparini, A.C. dos Santos, T. de Sousa Luz, M.C.S. de Macêdo, A study on the intergranular corrosion and pitting resistance of Inconel 625 coating by PTA-P, Corros. Eng. Sci. Technol. 54 (2019) 62–74. https://doi.org/10.1080/1478422X.2018.1533677.
[8] A.X. dos Santos, T.M. Maciel, J.D. Costa, M.B. de Sousa, S. Prasad, et al., Study on influence of the PTA-P welding process parameters on corrosion behavior of Inconel 625 coatings, Matéria. 24 (2019) e0619. https://doi.org/10.1590/S1517-707620190001.0619.
[9] C.P. Alvarães, F.C.A. Madalena, L.F.G. de Souza, J.C.F. Jorge, L.S. Araújo, M.C. Mendes, Performance of the Inconel 625 alloy weld overlay obtained by FCAW process, Matéria. 24 (2019) e12290. https://doi.org/10.1590/S1517-707620190001.0627.
[10] L. Guo, H. Zheng, S. Liu, Y. Li, X. Xu, C. Feng, Formation quality optimization and corrosion performance of Inconel 625 weld overlay using hot wire pulsed TIG, Rare Met. Mater. Eng. 45 (2016) 2219–2226. https://doi.org/10.1016/S1875-5372(17)30006-1.
[11] M.J. Moradi, M. Ketabchi, An experimental study of microstructure and mechanical behavior of Alloy 625 weld overlay deposited on

ASTM A516 Grade 70, Indian J. Sci. Technol. 8 (2015) 1–6. https://doi.org/10.17485/ijst/2015/v8i12/70725.
[12] P. Elango, S. Balaguru, Welding parameters for Inconel 625 overlay on carbon steel using GMAW, Indian J. Sci. Technol. 8 (2015) 1–5. https://doi.org/10.17485/ijst/2015/v8i31/84309.
[13] A. Kourdani, R.D. Haghighi, Evaluating the properties of dissimilar metal welding between Inconel 625 and 316L stainless steel by applying different welding methods and consumables, Metall. Mater. Trans. A. 49 (2018) 1453–1467. https://doi.org/10.1007/s11661-018-4469-7.
[14] M. Kumar, R. Shrimali, A.K. Singh, S. Pandey, Effect of welding current and electrode polarity on weld bead geometry and shape relationships in gravity-assisted mechanized contact shielded metal arc welding, Recent Advances, Materials and Manufacturing, Springer. (2024) 215–225. https://doi.org/10.1007/978-981-97-3654-6_22.
[15] A. Aloraier, K. Al-Fadhalah, A.M. Paradowska, E. Alfaraj, Effect of welding polarity on bead geometry, microstructure, microhardness, and residual stresses of 1020 steel, J. Eng. Res. 2 (2014) 137–160. https://doi.org/10.7603/s40632-014-0029-5.
[16] J.-S. Kim, Y.-I. Park, H.-W. Lee, Effects of heat input on the pitting resistance of Inconel 625 welds by overlay welding, Met. Mater. Int. 21 (2015) 350–355. https://doi.org/10.1007/s12540-015-4245-9.
[17] L. Xu, C. Shao, L. Tian, J. Zhang, Y. Han, et al., Intergranular corrosion behavior of Inconel 625 deposited by CMT/GTAW, Corros. Sci. 201 (2022) 110295. https://doi.org/10.1016/j.corsci.2022.110295.
[18] H. Kumar, G. Suresh, M. Krishnamoorthy, Microstructural evaluation and corrosion behaviour of Inconel 82 and Inconel 625 overlays on 304L stainless steel weld used in nuclear fuel reprocessing plant, Proc. Inst. Mech. Eng. L: J. Mater. Des. Appl. 238 (2024) 1358–1367. https://doi.org/10.1177/14644207231224169.
[19] V.B. Trindade, E.S. Souza, J.M.A. de Paula, M.C.M. de Souza Costa, G.L. de Faria, Effect of different heat treatments on microstructure and microhardness of a C-Mn steel/Inconel 625 coating system, Technol. Metal. Mater. Min. 14 (2017) 167–174. https://doi.org/10.4322/2176-1523.1182.
[20] T.J. Antoszczyszyn, R.M.G. Paes, A.S.C.M. de Oliveira, A. Scheid, Impact of dilution on the microstructure and properties of Ni-based 625 alloy coatings, Soldag. Inspeção. 19 (2014) 134–144. https://doi.org/10.1590/0104-9224/SI1902.05.
[21] K. Song, Z.-J. Wang, S. Hu, S. Zhang, E. Liang, Welding current influences on Inconel 625/X65 cladding interface, Mater. Manuf. Process. 33 (2018) 770–777. https://doi.org/10.1080/10426914.2017.1364851.
[22] P.K. Nachimuthu, S. Gosipathala, R.K. Arasappan, S.S. Nallathambi, High temperature corrosion performance of Inconel 625 hard overlays deposited on stainless steel substrate, Mater. Corros. 75 (2024) 875–890. https://doi.org/10.1002/maco.202314032.
[23] American Welding Society (AWS), Welding Handbook, 9th ed., Vol. 4, Materials and Applications, Part 1, American Welding Society, Miami, FL. (2011).
[24] B.-C. Goo, J.-W. Seo, Y.-J. Lee, Effect of welding polarity on mechanical properties of submerged arc welded railway vehicle wheels, Metals. 12 (2022) 1381. https://doi.org/10.3390/met12081381.
[25] L. Dong, Z. Shi, Y. Zhang, S. Wang, Q. Wang, L. Liu, Microstructure and sulfide stress corrosion cracking of the Inconel 625/X80 weld overlay fabricated by cold metal transfer process, Int. J. Hydrog. Energy. 47 (2022) 29113–29130. https://doi.org/10.1016/j.ijhydene.2022.06.210.
[26] J. Li, C. Li, S. Guo, L. Cheng, Y. Lei, et al., Degradation mechanism of hot corrosion resistance in Inconel 625 arc cladding layers induced by substrate Fe dilution in molten salt, Mater. Lett. 421 (2026) 141101. https://doi.org/10.1016/j.matlet.2026.141101.
[27] D. Ferreira Filho, D. Souza, J.L. Gonçalves Júnior, R.P. Reis, W.M. da Silva Junior, A.F. Tavares, Influence of substrate on the tribological behavior of Inconel 625 GMAW overlays, Coatings. 13 (2023) 1454. https://doi.org/10.3390/coatings13081454.